Bulletin of Mathematical Biology (2022) 84:146
https://doi.org/10.1007/s11538-022-01105-4

Society for Mathematical Biology

ORIGINAL ARTICLE

Analysis of a COVID-19 Epidemic Model with Seasonality

Zhimin Li[1] · **Tailei Zhang**[2]

Received: 21 July 2022 / Accepted: 2 November 2022 / Published online: 11 November 2022

Abstract
The statistics of COVID-19 cases exhibits seasonal fluctuations in many countries. In this paper, we propose a COVID-19 epidemic model with seasonality and define the basic reproduction number $\mathcal{R}_0$ for the disease transmission. It is proved that the disease-free equilibrium is globally asymptotically stable when $\mathcal{R}_0 < 1$, while the disease is uniformly persistent and there exists at least one positive periodic solution when $\mathcal{R}_0 > 1$. Numerically, we observe that there is a globally asymptotically stable positive periodic solution in the case of $\mathcal{R}_0 > 1$. Further, we conduct a case study of the COVID-19 transmission in the USA by using statistical data.

Keywords COVID-19 · Seasonal pattern · Basic reproduction number · Effective reproduction number · Threshold dynamics

1 Introduction

Coronavirus disease (COVID-19) is caused by infection with a newly discovered corona virus named the severe acute respiratory syndrome coronavirus 2 (SARS-CoV-2) virus strain. The virus is mainly transmitted by contacting saliva drops or secretions of infected people. The reported data from the World Health Organization (WHO) reported that the cumulative number of COVID-19 new cases by the end of June 2022 was over 547 million, including over 6.3 million deaths worldwide [15]. For control and prevention of the spread of COVID-19, many governments have implemented very strict epidemic prevention and control policies, such as keeping social distance, contact tracing, travel restrictions, self-isolation, medical quarantine, and even lockdown of living places.

✉ Zhimin Li
zhiminl@mun.ca

[1] Department of Mathematics and Statistics, Memorial University of Newfoundland, St. John's, NL A1C 5S7, Canada

[2] School of Science, Chang'an University, Xi'an 710064, China

There are many mathematical models of COVID-19 with the compartmental structure describing the size of populations within different classes (see Xue et al. 2020; Yan et al. 2020; Liu et al. 2021; Musa et al. 2022; Wang et al. 2022; Zou et al. 2022; Zhou et al. 2022; Zhang and Li 2021; Li et al. 2021; Tang et al. 2020a, b; Yang et al. 2020; Zhang et al. 2020; Munayco et al. 2020; Liu et al. 2020; Lauer et al. 2020; Kuniya 2020; Hu et al. 2020; Gatto et al. 2020). Xue et al. (2020) presented a data-driven network model to capture the contact heterogeneity between individuals. They used the Markov Chain Monte Carlo (MCMC) optimization algorithm to estimate the values of parameters and further applied the model to analyze the transmission potential and mitigation strategies of the COVID-19 epidemic in Wuhan, China, and Toronto, Canada, and the Republic of Italy. In Yan et al. (2020), Yan et al. proposed an epidemic model to show that media reports play an increasingly important role in the COVID-19 outbreak and analyzed the impact of media reports on the epidemic in some regions of China via statistical data. They also pointed out that media reports may provide the public with epidemic information and effective control measures to guide people's behavior changes to control the spread of the epidemic.

COVID-19 has lasted for nearly three years, and the case statistics indicates seasonal fluctuations in many countries. Liu et al. (2021) numerically studied the role of seasonality in the spread of COVID-19 pandemic by using a compartmental model and early statistical data. In this paper, we propose a time-periodic compartmental model to study the seasonality of COVID-19 based on the disease with incubation period and isolation policies. Since the most relevant parameter with seasonality is the transmission rate, we introduce a periodic transmission rate $\beta(t)$ between a susceptible and a symptomatic individual. We divide the infected population into symptomatic $I(t)$ and asymptomatic $A(t)$. During the epidemic, the potential contact population needs to be quarantined. Part of the quarantined population and infected population need to be isolated, so we introduce quarantined $Q(t)$ and isolated $J(t)$ classes into the model. Then, we define the basic reproduction number $\mathcal{R}_0$ to analyze the global dynamics of the model. In particular, we prove that as long as one of $A(t)$ and $I(t)$ is greater than 0 at some time t, the epidemic will break out, which extends the previous conclusion that the disease will be persistent only if both are greater than 0. Numerically, we study the COVID-19 transmission in the USA and investigate the seasonal spread of the disease by using the statistical data from the beginning of 2020 to the end of May 2022. Moreover, we introduce the effective reproduction number $\mathcal{R}_t$ to illustrate the scale of the epidemic over time via numerical simulations.

The rest of the paper is organized as follows. In Sect. 2, we present the model and study its well-posedness. In Sect. 3, we derive the basic reproduction number $\mathcal{R}_0$ and the effective reproduction number $\mathcal{R}_t$. We then establish a threshold type result on the global dynamics in terms of $\mathcal{R}_0$. In Sect. 4, we conduct a case study for COVID-19 transmission in USA. A brief discussion then concludes the paper.

2 The Model

In this section, we formulate a time-periodic COVID-19 epidemic model based on the possible fact that there is a seasonal trend for new COVID-19 cases. In view of the

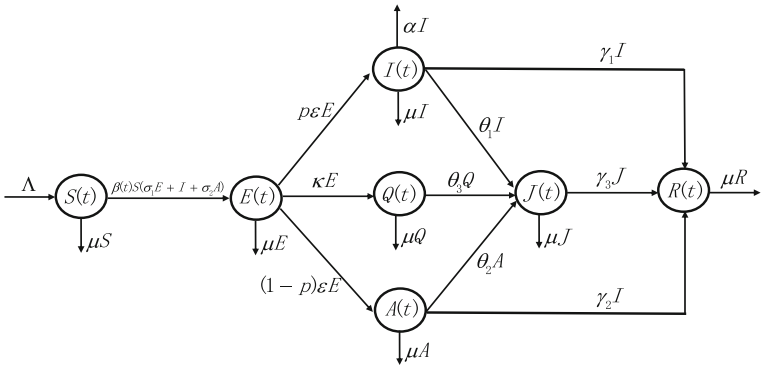

Fig. 1 Schematic flow diagram for the COVID-19 model. The model consists of seven sub-populations: susceptible $S(t)$, exposed $E(t)$, quarantined $Q(t)$, infectious with symptoms $I(t)$, asymptomatic infection $A(t)$, isolated $J(t)$ and recovered $R(t)$ individuals in a population of $N(t) = S(t) + E(t) + Q(t) + I(t) + A(t) + R(t)$ individuals

disease with incubation period and isolation policies, the total population is divided into seven sub-classes as follows:

- Susceptible individuals $S(t)$;
- Exposed individuals $E(t)$ who are exposed to the virus but not diagnosed positive for COVID-19 yet;
- Quarantined individuals $Q(t)$ refer to the separation of COVID-19 exposed individuals from the general population before the COVID-19 positive stage, for example, medical observation, self-quarantine, etc.;
- Infectious individuals with symptoms $I(t)$ who are confirmed COVID-19 positive patients and have clinical symptoms;
- Asymptomatic infection $A(t)$ who are confirmed COVID-19 positive patients and do not have clinical symptoms;
- Isolated individuals $J(t)$ who are confirmed COVID-19 positive patients and have been isolated, for example, by hospitalization, medical isolation, etc.;
- Recovered individuals $R(t)$.

The total population size is $N(t) = S(t) + E(t) + Q(t) + I(t) + A(t) + R(t)$. From (Wang et al. 2022), the COVID-19 virus is infectious in the incubation period. Based on the above population classification, the detailed transmission diagram is given in Fig. 1, and the model parameters and their definitions are shown in Table 1. In particular, we emphasize the relationship between compartments $E(t)$, $I(t)$, $A(t)$ and $Q(t)$, as shown in Fig. 2.

Therefore, the transmission process of COVID-19 is described by the following seven differential equations:

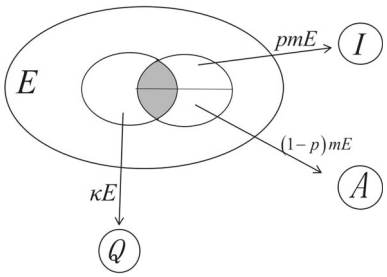

Fig. 2 The relationship between compartments $E(t)$, $I(t)$, $A(t)$ and $Q(t)$. For compartment $E(t)$, its pmE will become $I(t)$, $(1-p)mE$ will become $A(t)$, $pmE+(1-p)mE = mE$ will become COVID-19 positive and confirmed, and κE will become $Q(t)$. In particular, mE and κE may intersect (see shaded areas); that is, some individuals in compartment $Q(t)$ may be COVID-19 positive, and similarly, COVID-19 positive individuals may also belong to $Q(t)$

$$\begin{cases} \dfrac{\mathrm{d}S}{\mathrm{d}t} = \Lambda - \beta(t)S(\sigma_1 E + I + \sigma_2 A) - \mu S, \\ \dfrac{\mathrm{d}E}{\mathrm{d}t} = \beta(t)S(\sigma_1 E + I + \sigma_2 A) - (\mu + \kappa + m)E, \\ \dfrac{\mathrm{d}I}{\mathrm{d}t} = pmE - (\mu + \alpha + \theta_1 + \gamma_1)I, \\ \dfrac{\mathrm{d}A}{\mathrm{d}t} = (1-p)mE - (\mu + \theta_2 + \gamma_2)A, \\ \dfrac{\mathrm{d}Q}{\mathrm{d}t} = \kappa E - (\mu + \theta_3)Q, \\ \dfrac{\mathrm{d}J}{\mathrm{d}t} = \theta_1 I + \theta_2 A + \theta_3 Q - (\mu + s + \gamma_3)J, \\ \dfrac{\mathrm{d}R}{\mathrm{d}t} = \gamma_1 I + \gamma_2 A + \gamma_3 J - \mu R, \end{cases} \tag{1}$$

where all parameters are positive constant.

Here, we assume that $\beta(t)$ is a continuous positive periodic function in t with period ω for some $\omega > 0$ (ω can usually be chosen as 365-days, 52-weeks, 12-months according to actual scenario or case reported data structure, etc.). In fact, due to seasonal influence, β usually takes the form of $\beta(t) = \beta_0(1 + b\cos(\frac{2\pi}{\omega}t + \phi))$(see Zhang and Zhao 2007) to describe the transmission rate from a symptomatic patient to a susceptible individual, where positive constants β_0, b and ϕ represent the COVID-19 baseline transmission rate, its magnitude of forcing and the initial phase, respectively. Such seasonal function is also adopted in Liu et al. (2021).

In view of the biological interpretations, we denote by Γ the set

$$\Gamma = \left\{ (S, E, I, A, Q, J, R) \in \mathbb{R}^7_+ : S + E + I + A + Q + J + R \leq \frac{\Lambda}{\mu} \right\}.$$

By the expressions in system (2.1) and the comparison principle, it is easy to prove the following result.

Table 1 Descriptions of parameters in model (2.1)

Parameters	Description
Λ	Recruitment rate
μ	Natural mortality rate
$\beta(t)$	Basic transmission rate between a susceptible and a symptomatic individual
σ_1	Modification factor of transmission rate for exposed individuals
σ_2	Modification factor of transmission rate for asymptomatic individuals
m	Transition rate from exposed to infectious
p	Proportion of the exposed developing infected with symptoms
κ	Quarantined rate for exposed individuals
α	Disease-induced mortality rate for I
s	Disease-induced mortality rate for J
θ_1	Transition rate from symptomatic infected to isolated
θ_2	Transition rate from asymptomatic infected to isolated
θ_3	Transition rate from quarantined to isolated
γ_1	Recovery rate of symptomatic infected individuals
γ_2	Recovery rate of asymptomatic infected individuals
γ_3	Recovery rate of isolated individuals

Theorem 2.1 *For any $t_0 \in \mathbb{R}$ and each initial value $\mathbf{u}_0 = (S_0, E_0, I_0, A_0, Q_0, J_0, R_0) \in \Gamma$, system (2.1) admits a unique nonnegative solution*

$$\mathbf{u}(t, \mathbf{u}_0) = (S(t, \mathbf{u}_0), E(t, \mathbf{u}_0), I(t, \mathbf{u}_0), A(t, \mathbf{u}_0), Q(t, \mathbf{u}_0), J(t, \mathbf{u}_0), R(t, \mathbf{u}_0))$$

through $(t_0, \mathbf{u}_0)$ such that $\mathbf{u}(t, \mathbf{u}_0) \in \Gamma$ for all $t \geq t_0$. Moreover, all solutions are ultimately bounded.

3 Threshold Dynamics

In this section, we first introduce the basic reproduction number $\mathcal{R}_0$ for system (2.1) and then study the extinction and uniform persistence of the disease.

It is easy to see that system (2.1) has exactly one disease-free equilibrium $\mathbf{M}_0 = (\frac{\Lambda}{\mu}, 0, 0, 0, 0, 0, 0)$. Linearizing system (2.1) at the disease-free equilibrium $\mathbf{M}_0$, we then obtain the following linear periodic subsystem for the infective classes

$$\begin{cases} \dfrac{\mathrm{d}E}{\mathrm{d}t} = \beta(t)\dfrac{\Lambda}{\mu}(\sigma_1 E + I + \sigma_2 A) - (\mu + \kappa + m)E, \\ \dfrac{\mathrm{d}I}{\mathrm{d}t} = pmE - (\mu + \alpha + \theta_1 + \gamma_1)I, \\ \dfrac{\mathrm{d}A}{\mathrm{d}t} = (1-p)mE - (\mu + \theta_2 + \gamma_2)A. \end{cases} \tag{2}$$

We introduce

$$F(t) = \begin{pmatrix} \sigma_1\beta(t)\frac{\Lambda}{\mu} & \beta(t)\frac{\Lambda}{\mu} & \sigma_2\beta(t)\frac{\Lambda}{\mu} \\ 0 & 0 & 0 \\ 0 & 0 & 0 \end{pmatrix}$$

and

$$V(t) = \begin{pmatrix} \mu+\kappa+m & 0 & 0 \\ -pm & \mu+\alpha+\theta_1+\gamma_1 & 0 \\ -(1-p)m & 0 & \mu+\theta_2+\gamma_2 \end{pmatrix}.$$

Let $\Phi_V(t)$ and $\rho(\Phi_V(\omega))$ be the monodromy matrix of the linear ω-periodic system $x_t = V(t)x$ and the spectral radius of $\Phi_V(\omega)$, respectively. Assume that $Z(t,s)$, $t \geq s$, is a 3×3 matrix-valued solution of the system as follows:

$$\frac{\partial Z(t,s)}{\partial t} = -V(t)Z(t,s), \quad \forall t \geq s, \quad Z(s,s) = \mathbf{E}$$

where $\mathbf{E}$ is the 3×3 identity matrix.

Let C_ω be the ordered Banach space of all $\omega-$periodic functions from $\mathbb{R} \to \mathbb{R}^3$ with maximum norm $\|\cdot\|$. Let C_ω^+ be the positive cone $\{\varphi \in C_\omega : \varphi(t) \geq 0 \text{ for all } t \in \mathbb{R}\}$. Following (Wang and Zhao 2008), we define a linear operator $\mathcal{L} : C_\omega \to C_\omega$ as follows:

$$(\mathcal{L}\varphi)(t) = \int_0^\infty Z(t, t-a)F(t-a)\varphi(t-a)\mathrm{d}a, \ \forall t \in \mathbb{R}, \varphi \in C_\omega.$$

Naturally,

$$(\mathcal{L}\varphi)(t) = \int_{-\infty}^0 Z(t,s)F(s)\varphi(s)\mathrm{d}s, \ \forall t \in \mathbb{R}, \varphi \in C_\omega.$$

The operator $\mathcal{L}$ can be called the next infection operator and its spectral radius $\rho(\mathcal{L})$ can be defined as the basic reproduction number for system (2.1), that is

$$\mathcal{R}_0 = \rho(\mathcal{L}).$$

In order to estimate $\mathcal{R}_0$ in the periodic case, following (Wang and Zhao 2008), we let $U(t,\lambda)$ be the monodromy matrix of the following linear ω-periodic system

$$\frac{\mathrm{d}U}{\mathrm{d}t} = \left[\frac{F(t)}{\lambda} - V(t)\right]U(t) \tag{3}$$

with parameter $\lambda \in (0,\infty)$. Thus, we have the following results.

Lemma 3.1 (Wang and Zhao 2008, Theorem 2.1) *The following statements are valid.*

(1) If $\rho(U(\omega,\lambda)) = 1$ has a positive root λ_0, then λ_0 is an eigenvalue of $\mathcal{L}$, and hence, $\mathcal{R}_0 = 0$.
(2) If $\mathcal{R}_0 > 0$, then $\lambda = \mathcal{R}_0$ is the unique root of $\rho(U(\omega,\lambda)) = 1$.
(3) $\mathcal{R}_0 = 0$ if and only if $\rho(U(\omega,\lambda)) < 1$ for all $\lambda > 0$.

Using Lemma 3.1, we know $\mathcal{R}_0$ is the unique solution of $\rho(U(\omega,\lambda)) = 1$. Hence, the basic reproduction number $\mathcal{R}_0$ can be estimated by the numerical solution of the equation. On the local asymptotic stability of the disease-free periodic solution $P_0(t)$, the following results can be deduced from Theorem 2.2 in Wang and Zhao (2008).

Lemma 3.2 *The following statement are valid.*

(i) $\mathcal{R}_0 = 1$ if and only if $\rho(\Phi_{F-V}(\omega)) = 1$;
(ii) $\mathcal{R}_0 > 1$ if and only if $\rho(\Phi_{F-V}(\omega)) > 1$;
(iii) $\mathcal{R}_0 < 1$ if and only if $\rho(\Phi_{F-V}(\omega)) < 1$.

Therefore, the disease-free equilibrium $\mathbf{M}_0$ is locally asymptotically stable when $\mathcal{R}_0 < 1$ and unstable when $\mathcal{R}_0 > 1$, where $\Phi_{F-V}(t)$ is the monodromy matrix of the linear periodic system (3.2).

In the special case of $\beta(t) \equiv \beta$ for $\forall t \geq 0$, we obtain $F(t) \equiv F$. From (van den Driessche and Watmough 2002) and (Wang and Zhao 2008, Lemma 2.2(ii)), we can obtain the expression of the basic reproduction number $[\mathcal{R}_0]$ for the autonomous system of (2.1) as follows

$$[\mathcal{R}_0] = \beta\frac{\Lambda}{\mu}\left(\sigma_1 + \frac{pm}{\mu+\alpha+\theta_1+\gamma_1} + \frac{(1-p)m}{\mu+\theta_2+\gamma_2}\right).$$

Following (Wu et al. 2020), we then define the effective reproduction number of (2.1).

Definition 3.1 The effective reproduction number at time t is

$$\mathcal{R}_t = \beta(t)\frac{\Lambda}{\mu}\left(\sigma_1 + \frac{pm}{\mu+\alpha+\theta_1+\gamma_1} + \frac{(1-p)m}{\mu+\theta_2+\gamma_2}\right).$$

Theorem 3.1 *If $\mathcal{R}_0 < 1$, then the disease-free equilibrium $\mathbf{M}_0 = (\frac{\Lambda}{\mu}, 0, 0, 0, 0, 0, 0)$ is globally asymptotically stable*

Proof It is enough to verify that $\mathbf{M}_0$ is globally attractive as $\mathcal{R}_0 < 1$. Let $B_\epsilon(t) = F_\epsilon(t) - V(t)$ with

$$F_\epsilon(t) = \begin{pmatrix} \sigma_1\beta(t)(\frac{\Lambda}{\mu}+\epsilon) & \beta(t)(\frac{\Lambda}{\mu}+\epsilon) & \sigma_2\beta(t)(\frac{\Lambda}{\mu}+\epsilon) \\ 0 & 0 & 0 \\ 0 & 0 & 0 \end{pmatrix}.$$

By Lemma 3.2, when $\mathcal{R}_0 < 1$, the inequality $\rho(\Phi_{F-V}(\omega)) < 1$ holds. We can choose a sufficiently small $\epsilon > 0$ satisfying $\rho(\Phi_{B_\epsilon}(\omega)) < 1$.

Since the total population $N(t)$ satisfies the following differential system

$$\frac{\mathrm{d}N}{\mathrm{d}t} = \Lambda - \mu N(t) - \alpha I(t) \leq \Lambda - \mu N(t), \tag{4}$$

the comparison principle implies that there exist a $T_1 > 0$ such that $N(t) \leq \frac{\Lambda}{\mu} + \epsilon$ for all $t \geq T_1$. Thus, when $t \geq T_1$, one has

$$\begin{cases} \dfrac{\mathrm{d}E}{\mathrm{d}t} \leq \beta(t)(\dfrac{\Lambda}{\mu} + \epsilon)(\sigma_1 E + I + \sigma_2 A) - (\mu + \kappa + m)E, \\ \dfrac{\mathrm{d}I}{\mathrm{d}t} \leq pmE - (\mu + \alpha + \theta_1 + \gamma_1)I, \\ \dfrac{\mathrm{d}A}{\mathrm{d}t} \leq (1-p)mE - (\mu + \theta_2 + \gamma_2)A. \end{cases} \tag{5}$$

By (Zhang and Zhao 2007, Lemma 2.1), the system $\dfrac{\mathrm{d}\mathbf{u}}{\mathrm{d}t} = B_\epsilon(t)\mathbf{u}$ admits a positive ω-periodic solution $\mathbf{u}(t) = e^{pt}\mathbf{v}(t)$, where $\mathbf{v}(t)$ is a vector-valued ω-periodic function and $p = \frac{1}{\omega}\ln\rho(\Phi_{B_\epsilon}(\omega)) < 0$. It is immediate that $\mathbf{u}(t) \to \mathbf{0}$ as $t \to \infty$. According to the standard comparison principle, we deduce that

$$\lim_{t\to\infty}(E(t), I(t), A(t)) = (0, 0, 0).$$

By the theory of asymptotically periodic semi-flow (see (Zhao 2017, Theorem 3.2.1)), it can be concluded that

$$\lim_{t\to\infty}\left(S(t) - \frac{\Lambda}{\mu}, Q(t), J(t), R(t)\right) = (0, 0, 0, 0).$$

The proof is completed. □

Lemma 3.3 *Let* $\mathbf{u} = (\mathbf{u}_i(t, \mathbf{u}_0))$ $(i = 1, 2, \cdots, 7)$ *be the solution of system (2.1) with* $\mathbf{u}_0 \in \Gamma$. *If there exists some* $t_0 \geq 0$ *such that* $\mathbf{u}_i(t_0) > 0$ *for some* $i \in \{2, 3, 4\}$, *then* $\mathbf{u}_i(t) > 0$ *for both* $i = 2, 3, 4$ *with* $t > t_0$.

Proof If $I(t_0) > 0$ for some $t_0 \geq 0$, then $I(t)$ satisfies

$$\frac{\mathrm{d}I}{\mathrm{d}t} \geq -(\mu + \alpha + \theta_1 + \gamma_1)I,$$

and hence, $I(t) > 0$ for $\forall t > t_0$. It then follows the expression of E in system (2.1) and the positivity of S that $E(t) > 0$ for $\forall t > t_0$. By virtue of the expression of A in system (2.1), it is easy to see that $A(t) > 0$ for $\forall t > t_0$.

If $E(t_0) > 0$ for some $t_0 \geq 0$, then $E(t)$ satisfies

$$\frac{\mathrm{d}E}{\mathrm{d}t} \geq -(\mu + \kappa + m)E,$$

therefore, $E(t) > 0$ for $\forall t > t_0$. It then follows the expressions of I and A in system (2.1) that $I(t) > 0$ and $A(t) > 0$ for $\forall t > t_0$. It remains to show that when $A(t_0) > 0$ uses similar arguments in the first case. This proof is completed. □

Theorem 3.2 *If $\mathcal{R}_0 > 1$, then the disease is uniformly persistent, i.e., there exists a positive constant $\eta > 0$ such that any solution $(S(t), E(t), I(t), A(t), Q(t), J(t), R(t))$ in Γ of system (2.1) with $E(0) > 0$ or $I(0) > 0$ or $A(0) > 0$ satisfies*

$$\liminf_{t\to\infty} E(t) \geq \eta,\ \liminf_{t\to\infty} I(t) \geq \eta,\ \liminf_{t\to\infty} A(t) \geq \eta.$$

Moreover, system (2.1) admits at least one positive periodic solution as $\mathcal{R}_0 > 1$.

Proof Define

$$\begin{aligned} X &:= \Gamma, \\ X_0 &:= \{(S, E, I, A, Q, J, R) \in X : E > 0, I > 0 \text{ and } A > 0\}, \\ \partial X_0 &:= X \setminus X_0. \end{aligned}$$

Let $P(t) : \Gamma \to \Gamma$ be the solution map associated with system (2.1), and let $P := P(\omega)$ be the Poincaré map for this system, i.e.,

$$P(\mathbf{u}_0) = \mathbf{u}(\omega, \mathbf{u}_0),$$

where $\mathbf{u}(t, \mathbf{u}_0)$ is the unique solution of system (2.1) through $(0, \mathbf{u}_0)$. Next, we will show that system (2.1) is uniformly persistent. It is clear that both X and X_0 are positively invariant. The set ∂X_0 is relatively closed in X.

Write $\mathbf{u}_0 = (S_0, E_0, I_0, A_0, Q_0, J_0, R_0) \in X_0$. Let

$$u(t, \mathbf{u}_0) = (S(t, \mathbf{u}_0), E(t, \mathbf{u}_0), I(t, \mathbf{u}_0), A(t, \mathbf{u}_0), Q(t, \mathbf{u}_0), J(t, \mathbf{u}_0), R(t, \mathbf{y}_0))$$

be the solution of system (2.1) starting from $(0, \mathbf{u}_0)$.

By the continuity of solutions with respect to initial values, we have

$$\lim_{\mathbf{u}_0 \to \mathbf{M}_0} \|u(t, \mathbf{u}_0) - \mathbf{M}_0\| = 0$$

uniformly on $[0, \omega]$. Here, the symbol $\|\cdot\|$ denotes Euclidean distance on $\mathbb{R}^7$. Thus, for any $\epsilon > 0$, there exists a $\delta = \delta(\epsilon) > 0$, only dependent on ϵ, such that

$$\|u(t, \mathbf{u}_0) - \mathbf{M}_0\| < \epsilon,\ \forall t \in [0, \omega] \tag{6}$$

whenever $\|\mathbf{u}_0 - \mathbf{M}_0\| < \delta$. □

Claim 1. $\limsup_{n\to\infty} \|P^n(\mathbf{u}_0) - \mathbf{M}_0\| \geq \delta$ for each $\mathbf{u}_0 \in X_0$.

If the claim is not true, then there is a $\bar{\mathbf{u}}_0 \in X_0$ such that

$$\limsup_{n\to\infty} \|P^n(\bar{\mathbf{u}}_0) - \mathbf{M}_0\| < \delta.$$

Then, there exists a $n_0 \in \mathbb{N}$ such that $\|P^n(\bar{\mathbf{u}}_0) - \mathbf{M}_0\| < \delta$ for all $n \geq n_0$. Therefore,

$$\|u(t, P^n(\bar{\mathbf{u}}_0)) - \mathbf{M}_0\| < \epsilon, \ \forall t \in [0, \omega]$$

provided $n \geq n_0$. For any $t \geq n_0\omega$, letting $m = \left[\frac{t}{\omega}\right]$ which is the greatest integer less than or equal to $\frac{t}{\omega}$, we have $t = \bar{t} + m\omega$ with $\bar{t} \in [0, \omega)$ and $m \geq n_0$. It follows that

$$\|u(t, \bar{\mathbf{u}}_0) - \mathbf{M}_0\| = \|u(\bar{t}, P^m(\bar{\mathbf{u}}_0)) - \mathbf{M}_0\| < \epsilon \tag{7}$$

for all $t \geq n_0\omega$. This implies that

$$\begin{array}{c} |S(t, \bar{\mathbf{u}}_0) - \frac{\Lambda}{\mu}| < \epsilon, \ 0 < E(t, \bar{\mathbf{u}}_0) < \epsilon, \\ 0 < I(t, \bar{\mathbf{u}}_0) < \epsilon, 0 < A(t, \bar{\mathbf{u}}_0) < \epsilon \end{array} \tag{8}$$

for all $t \geq n_0\omega$.

From the second, third and fourth equations of system (2.1), when $t \geq n_0\omega$, $(E(t, \bar{\mathbf{u}}_0), I(t, \bar{\mathbf{u}}_0), A(t, \bar{\mathbf{u}}_0))$ satisfies the differential inequality as follows:

$$\begin{cases} \frac{\mathrm{d}E}{\mathrm{d}t} \geq \beta(t)(\frac{\Lambda}{\mu} - \epsilon)(\sigma_1 E + I + \sigma_2 A) - (\mu + \kappa + m)E, \\ \frac{\mathrm{d}I}{\mathrm{d}t} \geq pmE - (\mu + \alpha + \theta_1 + \gamma_1)I, \\ \frac{\mathrm{d}A}{\mathrm{d}t} \geq (1-p)mE - (\mu + \theta_2 + \gamma_2)A. \end{cases}$$

Consider the following auxiliary perturbed system

$$\begin{cases} \frac{\mathrm{d}\hat{E}}{\mathrm{d}t} = \beta(t)(\frac{\Lambda}{\mu} - \epsilon)(\sigma_1 \hat{E} + \hat{I} + \sigma_2 \hat{A}) - (\mu + \kappa + m)\hat{E}, \\ \frac{\mathrm{d}\hat{I}}{\mathrm{d}t} = pm\hat{E} - (\mu + \alpha + \theta_1 + \gamma_1)\hat{I}, \\ \frac{\mathrm{d}\hat{A}}{\mathrm{d}t} = (1-p)m\hat{E} - (\mu + \theta_2 + \gamma_2)\hat{A}. \end{cases} \tag{9}$$

Let

$$C_\epsilon(t) = \begin{pmatrix} \sigma_1\beta(t)(\frac{\Lambda}{\mu} - \epsilon) - (\mu + \kappa + m) & \beta(t)(\frac{\Lambda}{\mu} - \epsilon) & \sigma_2\beta(t)(\frac{\Lambda}{\mu} - \epsilon) \\ pm & -(\mu + \alpha + \theta_1 + \gamma_1) & 0 \\ (1-p)m & 0 & -(\mu + \theta_2 + \gamma_2) \end{pmatrix}$$

Since $\mathcal{R}_0 > 1$, one has $\rho(\Phi_{F-V}(\omega)) > 1$. Choose a sufficiently small $\epsilon > 0$ such that $\rho(\Phi_{C_\epsilon}(\omega)) > 1$. By (Zhang and Zhao 2007, Lemma 2.1), we know that there exists a positive, $\omega-$periodic function $(E^*(t), I^*(t), A^*(t))$ such that $(\hat{E}(t), \hat{I}(t), \hat{A}(t)) = e^{qt}(E^*(t), I^*(t), A^*(t))$ is a solution of system (3.8) where $q = \frac{1}{\omega}\ln\rho(\Phi_{C_\epsilon}(\omega)) > 0$. It is convenient to choose $\xi > 0$ satisfying

$(E(n_0\omega, \bar{\mathbf{u}}_0), I(n_0\omega, \bar{\mathbf{u}}_0), A(n_0\omega, \bar{\mathbf{u}}_0)) \geq \xi \cdot (\hat{E}(n_0\omega), \hat{I}(n_0\omega), \hat{A}(n_0\omega))$. By the comparison principle, it follows that $(E(t, \bar{\mathbf{u}}_0), I(t, \bar{\mathbf{u}}_0), A(t, \bar{\mathbf{u}}_0)) \geq \xi(\hat{E}(t), \hat{I}(t), \hat{A}(t))$ for all $t \geq n_0\omega$. We thus get

$$E(n\omega, \bar{\mathbf{u}}_0) \to \infty,\ I(n\omega, \bar{\mathbf{u}}_0) \to \infty,\ A(n\omega, \bar{\mathbf{u}}_0) \to \infty$$

as $n \to \infty$. This contradicts the boundedness of solutions of system (2.1). In this way, this claim is valid.

Claim 1 implies that $\mathbf{M}_0$ is an isolated invariant set for Poincaré mapping P in X, and $\mathrm{W}^s(\mathbf{M}_0) \bigcap X_0 = \emptyset$, where $\mathrm{W}^s(\mathbf{M}_0)$ is the stable set of $\mathbf{M}_0$ for P. Define

$$M_\partial := \{\mathbf{u}_0 \in \partial X_0 : P^n(\mathbf{u}_0) \in \partial X_0,\ \forall n \in \mathbb{N}\},$$

and $\omega(\mathbf{u}_0)$ be the omega limit set of the forward orbit $\gamma^+(\mathbf{u}_0) = \{P^n(\mathbf{u}_0) : \forall n \in \mathbb{N}\}$ of (2.1). Then, we prove the following claim.

Claim 2 $\mathbf{M}_0$ is globally stable for P in M_∂.

Let $\overline{M_\partial} := \{\mathbf{u}_0 \in X : E = I = A = 0\}$. We first show that $M_\partial = \overline{M_\partial}$. Clearly, $\overline{M_\partial} \subset M_\partial$. It then suffices to prove that $M_\partial \subset \overline{M_\partial}$, that is, it suffices to prove that for any $\mathbf{u}_0 \in M_\partial$, the solution $\mathbf{u}(t, \mathbf{u}_0) = (S(t, \mathbf{u}_0), E(t, \mathbf{u}_0), I(t, \mathbf{u}_0), A(t, \mathbf{u}_0), Q(t, \mathbf{u}_0), J(t, \mathbf{u}_0), R(t, \mathbf{u}_0))$ through $(0, \mathbf{u}_0)$ satisfies $E(t, \mathbf{u}_0) = I(t, \mathbf{u}_0) = A(t, \mathbf{u}_0) = 0$ for each $t \geq 0$. If it is not true, there exists a $t^* > 0$ such that $E(t^*, \mathbf{u}_0) > 0$ or $I(t^*, \mathbf{u}_0) > 0$ or $A(t^*, \mathbf{u}_0) > 0$. We give the proof only for the case $I(t^*, \mathbf{u}_0) > 0$, the other case can be handled in the same way. The inequality $I'(t) \geq -(\mu + \alpha + \theta_1 + \gamma_1)I(t)$ implies that $I(t, \mathbf{u}_0) > 0$ for all $t \geq t^*$.

From the first equation of system (2.1), we have

$$\begin{aligned} S(t) &= S(0)e^{-\int_0^t b(\xi)\mathrm{d}\xi} + \Lambda e^{-\int_0^t b(\xi)\mathrm{d}\xi} \int_0^t e^{\int_0^\xi b(\rho)\mathrm{d}\rho}\mathrm{d}\xi \\ &\geq \Lambda e^{-\int_0^t b(\xi)\mathrm{d}\xi} \int_0^t e^{\int_0^\xi b(\rho)\mathrm{d}\rho}\mathrm{d}\xi > 0 \end{aligned} \tag{10}$$

for all $t > 0$, where $b(t) = \mu + \beta(t)[\sigma_1 E(t) + I(t) + \sigma_2 A(t)]$. Hence, from the second and third equations of (2.1), we obtain

$$E(t, \mathbf{u}_0) \geq E(t^*, \mathbf{u}_0)e^{-(\mu+\kappa+m)t} + \int_{t^*}^t \sigma_1\beta(\xi)I(\xi, \mathbf{u}_0)e^{-(\mu+\kappa+m)(t-\xi)}\mathrm{d}\xi > 0$$

and

$$A(t, \mathbf{u}_0) \geq A(t^*, \mathbf{u}_0)e^{-(\mu+\theta_2+\gamma_2)t} + \int_{t^*}^t (1-p)mE(\xi, \mathbf{u}_0)e^{-(\mu+\theta_2+\gamma_2)(t-\xi)}\mathrm{d}\xi > 0$$

for all $t > t^*$. This gives $\mathbf{u}(t, \mathbf{u}_0) \in X_0$ for each $t > t^*$, contrary to $\mathbf{u}_0 \in M_\partial$.

Next we prove that the omega limit set $\omega(\mathbf{u}_0) = \mathbf{M}_0$ for any $\mathbf{u}_0 \in M_\partial$. Since $M_\partial = \overline{M_\partial}$, we have $E(t, \mathbf{u}_0) = I(t, \mathbf{u}_0) = A(t, \mathbf{u}_0) = 0$ for all $\mathbf{u}_0 \in \overline{M_\partial}$ and $t \geq 0$.

In view of system (2.1), it follows that S, Q, J and R satisfy the following system:

$$\begin{cases} \dfrac{\mathrm{d}S}{\mathrm{d}t} = \Lambda - \mu S, \\ \dfrac{\mathrm{d}Q}{\mathrm{d}t} = -(\mu + \theta_3)Q, \\ \dfrac{\mathrm{d}J}{\mathrm{d}t} = \theta_3 Q - (\mu + \gamma_3)J, \\ \dfrac{\mathrm{d}R}{\mathrm{d}t} = \gamma_3 J - \mu R, \end{cases} \tag{11}$$

and hence, $\lim_{t\to\infty}\left(S(t) - \frac{\Lambda}{\mu}, Q(t), J(t), R(t)\right) = (0, 0, 0, 0)$ uniformly. Therefore, $\omega(\mathbf{u}_0) = \mathbf{M}_0$ for any $\mathbf{u}_0 \in M_\partial$. This implies that $\mathbf{M}_0$ is globally attractive for P in M_∂. Since system (3.10) is cooperative, it follows from (Zhao 2017, Lemma 2.2.1) that $\mathbf{M}_0$ is locally Lyapunov stable for P in M_∂. This proves Claim 2 above.

By virtue of Claim 2, we obtain that $\bigcup_{\mathbf{u}_0\in M_\partial}\omega(\mathbf{u}_0) = \mathbf{M}_0$ and $\mathbf{M}_0$ cannot form a cycle for P in M_∂ (and hence in ∂X_0). Since P admits a global attractor on X due to all solutions are ultimately bounded from Theorem 2.1, it then follows from the acyclicity theorem on uniform persistence for maps [see (Zhao 2017, Theorem 1.3.1 and Remark 1.3.1)] that $P : X \to X$ is uniformly persistent with respect to $(X_0, \partial X_0)$. Thus, (Zhao 2017, Theorem 3.1.1) implies that the solution of (2.1) is uniformly persistent under $E(0) > 0$, $I(0) > 0$ and $A(0) > 0$.

If $E(0) > 0$ or $I(0) > 0$ or $A(0) > 0$, it follows from Lemma 3.3 that there exists an integer $n_0 \geq 0$ such that $P^{n_0}(\mathbf{u}_0) \in X_0$. Since $P(t)\mathbf{u}_0 = P(t - n_0\omega)\left(P^{n_0}(\mathbf{u}_0)\right), \forall t \geq n_0\omega$, the uniform persistence also holds.

By (Zhao 2017, Theorem 1.3.10), the Poincaré map P has a fixed point $(S^*(0), E^*(0), I^*(0), A^*(0), Q^*(0), J^*(0), R^*(0)) \in X_0$. The corresponding periodic solution is denoted by $(S^*(t), E^*(t), I^*(t), A^*(t), Q^*(t), J^*(t), R^*(t))$. By $E^*(0) > 0$, $I^*(0) > 0$ and $A^*(0) > 0$, it is obvious that $E^*(t) > 0$, $I^*(t) > 0$, $A^*(t) > 0$ for all $t \geq 0$. Furthermore, integrating the fifth equation of (2.1) yields

$$Q^*(t) = Q^*(0)e^{-(\mu+\theta_3)t} + \int_0^t \kappa E^*(\xi)e^{-(\mu+\theta_3)(t-\xi)}\mathrm{d}\xi > 0$$

for all $t > 0$. The periodicity of $Q^*(t)$ implies $Q^*(t) > 0$ for all $t \geq 0$. In the same manner, we can see that $S^*(t) > 0$, $J^*(t) > 0$, $R^*(t) > 0$ for all $t \geq 0$. Consequently, $(S^*(t), E^*(t), I^*(t), A^*(t), Q^*(t), J^*(t), R^*(t))$ is a positive ω-periodic solution of (2.1).

4 A Case Study

In this section, we first present some numerical simulations for the model and then use the reported data to investigate the impact of seasonality on the spread of the COVID-19 epidemic in the USA.

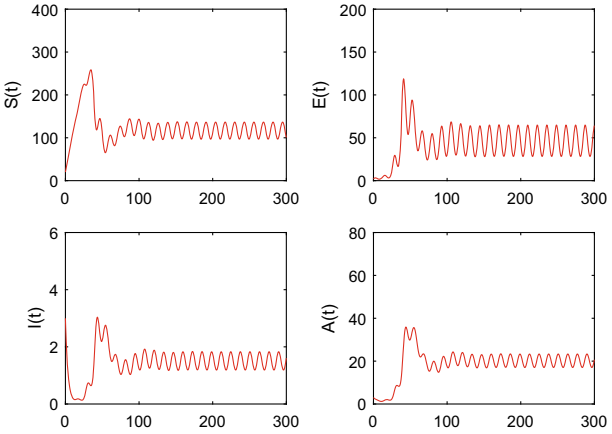

Fig. 3 (color figure online) The long-term behaviors of $S(t)$, $E(t)$, $I(t)$ and $A(t)$ population when $\mathcal{R}_0 = 11.4 > 1$

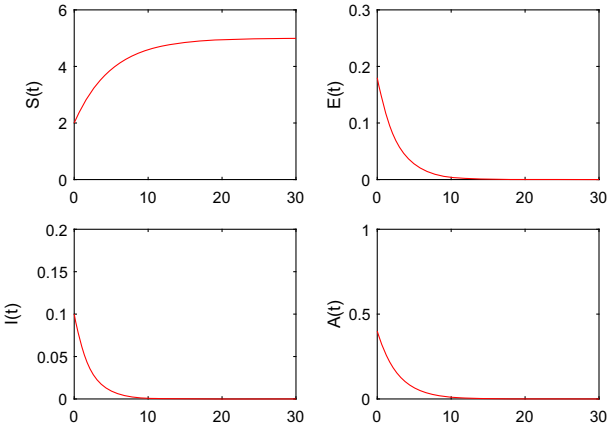

Fig. 4 (color figure online) The global asymptotic stability of the disease-free equilibrium $\mathbf{M}_0$ as $\mathcal{R}_0 = 0.01725 < 1$

4.1 Numerical Simulations of Dynamic Behavior

By virtue of Theorems 3.1 and 3.2, it is easy to see that $\mathcal{R}_0$ is a threshold parameter to determine whether or not COVID-19 persists in the population. Let $\beta_0 = 0.01$, $\Lambda = 10$, $\mu = 0.005$, $\sigma_1 = 0.1$, $\sigma_2 = 0.1$, $m = 0.1$, $p = 0.1$, $\alpha = 0.1$, $\theta_1 = 0.1$, $\theta_2 = 0.1$, $\gamma_1 = 0.1$, $\gamma_2 = 0.1$, $b_0 = 1$ and $\phi = \pi/6$, we get $\mathcal{R}_0 = 11.4$. The numerical results are illustrated in Fig. 3, and these are the same as Theorem 3.2, that is, the disease is persistent. Moreover, the numerical results also show that there exists a unique globally attractive positive periodic solution as $\mathcal{R}_0 = 11.4 > 1$. Then, we give $\Lambda = 1$, $\mu = 0.2$, $b_0 = 0.1$ and keep the values of other parameters unchanged to get $\mathcal{R}_0 = 0.01725$. This shows that the disease is extinct. As described in Theorem

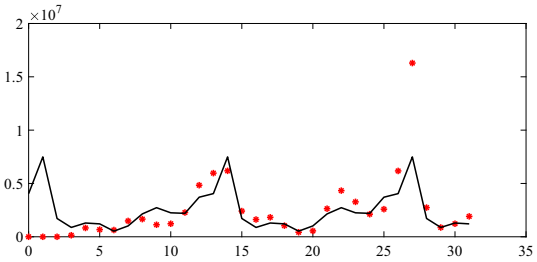

Fig. 5 Reported new COVID-19 cases and their fitted curve. From March 8th, 2020, each unit length of time represents 4 weeks (28 days)

3.1, there is a unique disease-free equilibrium $\mathbf{M}_0$ which is globally asymptotically stable when $\mathcal{R}_0 = 0.01725 < 1$, (see Fig. 4).

4.2 A Case Study of the COVID-19 in the USA

Since the end of 2019 when the COVID-19 epidemic broke out, the USA has the largest number of existing infection cases. The epidemic has lasted for nearly three years, according to statistical data analysis, the data of new infection cases show seasonal periodicity to some extent. To further explore the seasonality of the epidemic transmission, we collect the data [the data come from (https://www.arcgis.com/apps/opsdashboard/index.html)] of new COVID-19 cases from the outbreak of the epidemic in the USA in early 2020 to the end of May 2022, which are summarized in Table 2.

The new cases in Table 2 include symptomatic and asymptomatic infected individuals. Considering system (2.1), we easily obtain that the number of new COVID-19 cases corresponds to the term $pmE + (1-p)mE = mE$. Since variables and parameters in system (2.1) are continuous function of t, we use trigonometric functions to fit mE as a periodic function with period $\frac{365}{4\times 7} = 13$. This is because Table 2 is cumulative data for each week, so in the numerical simulation, the cumulative cases of four weeks are taken as a point; that is, $\frac{365}{4\times 7}$ is a period. We use MATLAB software to fit mE by the data in Table 2 to obtain the coefficients of trigonometric functions. The comparison of the data with the curve of mE is shown in Fig. 5. Obviously, these two match well, and the expression is obtained as follows:

$$\begin{aligned} mE = 2.40025 \times 10^6 \times \Bigg[& 1 + 0.684 \cos\left(\frac{2\pi t}{13} + \frac{\pi}{6}\right) + 0.241 \sin\left(\frac{2\pi t}{13} + \frac{\pi}{6}\right) \\ & + 0.122 \cos\left(\frac{4\pi t}{13} + \frac{\pi}{6}\right) + 0.399 \sin\left(\frac{4\pi t}{13} + \frac{\pi}{6}\right) \\ & + 0.122 \cos\left(\frac{6\pi t}{13} + \frac{\pi}{6}\right) + 0.403 \sin\left(\frac{6\pi t}{13} + \frac{\pi}{6}\right) \\ & - 0.228 \cos\left(\frac{8\pi t}{13} + \frac{\pi}{6}\right) + 0.141 \sin\left(\frac{8\pi t}{13} + \frac{\pi}{6}\right) \\ & - 0.268 \cos\left(\frac{10\pi t}{13} + \frac{\pi}{6}\right) + 0.0064 \sin\left(\frac{10\pi t}{13} + \frac{\pi}{6}\right) \end{aligned}$$

Table 2 New COVID-19 cases from the outbreak of the epidemic in the USA in early 2020 to the end of May 2022

Date	Cases	Date	Cases	Date	Cases	Date	Cases
2020/3/8	499	2020/9/27	284.778k	2021/4/18	480.084k	2021/11/7	517.581k
2020/3/15	2.696k	2020/10/4	300.503k	2021/4/25	404.688k	2021/11/14	561.197k
2020/3/22	31.71k	2020/10/11	346.277k	2021/5/2	346.015k	2021/11/21	656.049k
2020/3/29	108.6k	2020/10/18	391.358k	2021/5/9	286.679k	2021/11/28	509.969k
2020/4/5	205.472k	2020/10/25	490.957k	2021/5/16	233.408k	2021/12/5	859.505k
2020/4/12	218.006k	2020/11/1	584.577k	2021/5/23	177.801k	2021/12/12	832.487k
2020/4/19	196.864k	2020/11/8	808.71k	2021/5/30	140.807k	2021/12/19	949.492k
2020/4/26	207.182k	2020/11/15	1.043m	2021/6/6	101.721k	2021/12/26	1.447m
2020/5/3	191.166k	2020/11/22	1.21m	2021/6/13	100.036k	2022/1/2	2.944m
2020/5/10	170.426k	2020/11/29	1.176m	2021/6/20	81.341k	2022/1/9	5.107m
2020/5/17	155.994k	2020/12/6	1.405m	2021/6/27	87.083k	2022/1/16	5.649m
2020/5/24	154.981k	2020/12/13	1.53m	2021/7/4	91.024k	2022/1/23	4.944m
2020/5/31	144.932k	2020/12/20	1.552m	2021/7/11	141.683k	2022/1/30	3.536m
2020/6/7	149.555k	2020/12/27	1.318m	2021/7/18	231.58k	2022/2/6	1.997m
2020/6/14	149.833k	2021/1/3	1.567m	2021/7/25	370.348k	2022/2/13	1.24m
2020/6/21	189.541k	2021/1/10	1.744m	2021/8/1	570.405k	2022/2/20	698.779k
2020/6/28	276.805k	2021/1/17	1.53m	2021/8/8	768.025k	2022/2/27	464.446k
2020/7/5	346.363k	2021/1/24	1.88m	2021/8/15	922.787k	2022/3/6	334.064k
2020/7/12	409.787k	2021/1/31	1.03m	2021/8/22	1.043m	2022/3/13	241.234k
2020/7/19	451.592k	2021/2/7	829.15k	2021/8/29	1.095m	2022/3/20	212.742k
2020/7/26	459.474k	2021/2/14	639.883k	2021/9/5	1.164m	2022/3/27	218.515k
2020/8/2	427.186k	2021/2/21	460.301k	2021/9/12	1.026m	2022/4/3	196.742k
2020/8/9	396.656k	2021/2/28	480.121k	2021/9/19	1.019m	2022/4/10	244.031k

Table 2 continued

Date	Cases	Date	Cases	Date	Cases	Date	Cases
2020/8/16	372.655k	2021/3/7	415.374k	2021/9/26	843.642k	2022/4/17	237.433k
2020/8/23	298.938k	2021/3/14	377.859k	2021/10/3	748.276k	2022/4/24	354.567k
2020/8/30	292.89k	2021/3/21	382.643k	2021/10/10	661.767k	2022/5/1	384.809k
2020/9/6	281.518k	2021/3/28	442.412k	2021/10/17	583.005k	2022/5/8	507.185k
2020/9/13	254.89k	2021/4/4	450.775k	2021/10/24	498.109k	2022/5/15	603.725k
2020/9/20	290.926k	2021/4/11	488.5k	2021/10/31	518.611k	2022/5/22	799.759k

The data come from (https://www.arcgis.com/apps/opsdashboard/index.html)

Table 3 The values of some model parameters and the initial values of compartment variables

Symbol	Value	Source
Λ	290664 (28 days)$^{-1}$	See text
μ	$\frac{1}{78.6\times13}$ (28 days)$^{-1}$	See text
m	0.513	Estimated
α	0.0263	Khan et al. (2020)
γ_1	0.9937	Khan et al. (2020)
γ_2	0.9937	Khan et al. (2020)
σ_1	0.1974	Estimated
σ_2	0.6304	Estimated
k	0.9955	Estimated
p	0.6884	Estimated
θ_1	0.9955	Estimated
θ_2	0.9955	Estimated
$S(0)$	2.97×10^8	http://www.who.int/
$E(0)$	100	Estimated
$I(0)$	4	https://www.arcgis.com/apps/opsdashboard/index.html
$A(0)$	0	https://www.arcgis.com/apps/opsdashboard/index.html

$$-0.278\cos\left(\frac{12\pi t}{13}+\frac{\pi}{6}\right)-0.0855\sin\left(\frac{12\pi t}{13}+\frac{\pi}{6}\right)\Bigg].$$

The average life expectancy of the American was 78.6 years in 2019 (see http://www.who.int/). We take this number as the current average life expectancy, therefore, the natural mortality rate $\mu = \frac{1}{78.6\times13}$ (28 days)$^{-1}$. Note that, the recruitment rate is the product of the birth rate (equals to the natural death rate) and the total number of the whole population, the total population is 2.97×10^8 from [15], and hence, $\Lambda = \frac{2.97\times10^8}{78.6\times13} = 290664$ (28 days)$^{-1}$. Based on the obtained values of parameters and the initial values of compartment variables (see Table 3), applying them to model (2.1), and fitting the summarized data in Table 2 with the least square method, we get the fitted values of parameters with a high degree of agreement. These results are shown in Table 3. In particular, we get the expression of $\beta(t)$ as follows:

$$\begin{aligned}\beta(t) = 4.9794\times10^{-8}\times\Bigg[&1+0.09977\cos\left(\frac{2\pi t}{13}+\frac{\pi}{6}\right)-0.114\sin\left(\frac{2\pi t}{13}+\frac{\pi}{6}\right)\\&-0.0671\cos\left(\frac{4\pi t}{13}+\frac{\pi}{6}\right)+0.0742\sin\left(\frac{4\pi t}{13}+\frac{\pi}{6}\right)\\&-0.0671\cos\left(\frac{6\pi t}{13}+\frac{\pi}{6}\right)+0.1\sin\left(\frac{6\pi t}{13}+\frac{\pi}{6}\right)\\&-0.2597\cos\left(\frac{8\pi t}{13}+\frac{\pi}{6}\right)+0.1144\sin\left(\frac{8\pi t}{13}+\frac{\pi}{6}\right)\end{aligned}$$

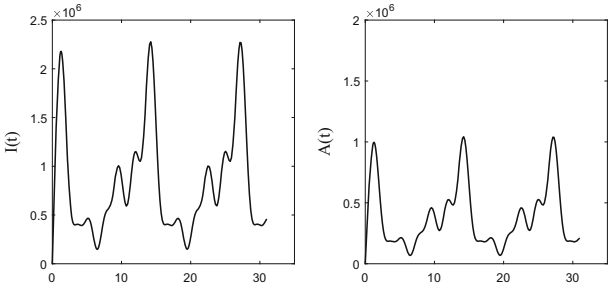

Fig. 6 From the fitting of the transmission of the COVID-19 in the USA, the evolution of $I(t)$ and $A(t)$ over time. From March 8th, 2020, each unit length of time represents 4 weeks (28 days)

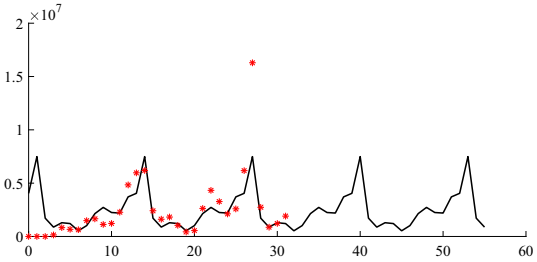

Fig. 7 Time 0 to 31 are the reported new COVID-19 cases and their fitted curve. After time 31, it means that if no control is adopted, the new COVID-19 cases will maintain such seasonal changes. Time 0 represents March 8th, 2020, each unit length of time represents 4 weeks (28 days)

$$-0.0671\cos\left(\frac{10\pi t}{13}+\frac{\pi}{6}\right)+0.0671\sin\left(\frac{10\pi t}{13}+\frac{\pi}{6}\right)$$
$$-0.0671\cos\left(\frac{12\pi t}{13}+\frac{\pi}{6}\right)+0.0672\sin\left(\frac{12\pi t}{13}+\frac{\pi}{6}\right)\Bigg].$$

The basic reproduction number is an important indicator to describe the outbreak degree of the epidemic. From the values in Table 3, we get $\mathcal{R}_0 = 6.69$ of the COVID-19 in the USA by numerical calculation. It then follows from those parameter values and $\beta(t)$ that some simulations of the epidemic in the USA. We take March 8th, 2020 as the initial time of the simulation. Each unit time length represents 4 weeks. From the fitting of the transmission for the disease in the USA, the evolution of $I(t)$ and $A(t)$ over time is shown in Fig. 6. In particular, if no control strategy is adopted, the epidemic will continue to occur seasonally, and the scale of new COVID-19 cases in the USA is illustrated in Fig. 7.

It is worth noting that in the above numerical simulations, since the size of the initial infected population is very small, we assume that the total population is susceptible and consider $S(0) = \frac{\Lambda}{\mu}$, and then calculate the basic reproduction number $\mathcal{R}_0$. However, with the continuous outbreak of COVID-19, the size of the susceptible population will decrease significantly due to the increase in the number of infected people. The value of the basic reproduction number cannot accurately describe the outbreak scale of the epidemic. Therefore, in the early stage of the outbreak of the disease, the basic reproduction number $\mathcal{R}_0$ can be used to describe the outbreak scale. If the complete epidemic data are used to estimate other parameters to calculate the basic reproduction number, it may not be accurate and cannot describe the risk at a certain time t. So, we

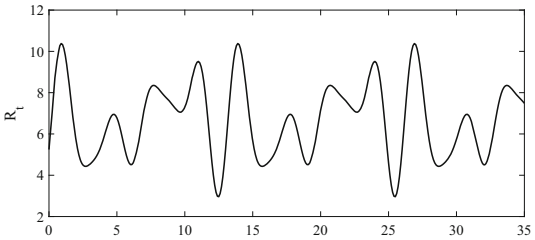

Fig. 8 Relationship between the effective reproduction number $\mathcal{R}_t$ and the time t. Time 0 represents March 8th, 2020, each unit length of time represents 4 weeks (28 days)

introduce the effective reproduction number $\mathcal{R}_t$ to describe the epidemic scale over time. In virtue of the obtained values of parameters and the expression of $\beta(t)$, it is easy to see that the effective reproduction number $\mathcal{R}_t$ as shown in Fig. 8.

5 Discussion

The COVID-19 pandemic puts epidemic modeling at the forefront of global public policy-making. Nevertheless, it is still very challenging to model and predict the spread of COVID-19. Especially for the specific model, the parameters of the model are fitted by using statistical data, so that the model with known parameters can be applied to describe the actual spread of the epidemic, which can give some scientific evaluation and prediction. In this paper, we use a time-periodic compartmental model to describe the COVID-19 seasonal transmission rate. We find that there is a seasonal pattern of the new COVID-19 cases, and the numbers of the peak value of new cases are from November of the current year to February of the following year, and reach a nadir from May to June in the USA (see Fig. 5). This seasonal pattern may be related to new year's day and Christmas. During the festivals, people travel and frequent social activities, which lead to the virus's rapid spread. Furthermore, winter and spring are the peaks of influenza outbreaks, reducing people's immunity, which may also be the reason for the COVID-19 peak.

We illustrate that the basic reproduction number $\mathcal{R}_0$ serves as a threshold value for the extinction and persistent of the disease. More precisely, if $\mathcal{R}_0 < 1$, then the unique disease-free equilibrium is globally asymptotically stable (see Theorem 3.1 and Fig. 4); while the disease is uniformly persistent and there exists at least one positive periodic solution if $\mathcal{R}_0 > 1$ (see Theorem 3.2 and Fig. 3). Numerical simulations show that there is only one positive periodic solution that is globally asymptotically stable as $\mathcal{R}_0 > 1$ (see Fig. 3). Figure 5 indicates that the fitted curve of new COVID-19 cases matches the statistical data very well. The expression of $\beta(t)$ and other parameters are further estimated by the least square method, and $\mathcal{R}_0 = 6.69$ is obtained via numerical calculation. The numerical results illustrate that if no measures are taken, the epidemic in the USA will continue to break out, as shown in Fig. 7. It is not always reasonable to use $\mathcal{R}_0$ to describe the outbreak of the whole epidemic. In order to describe the change of the epidemic situation over time, we introduce the effective reproduction number $\mathcal{R}_t$, its change with time as shown in Fig. 8.

Acknowledgements Li was partially supported by the NSERC of Canada (RGPIN-2019-05648). Zhang was partially supported by the Natural Science Basic Research Plan in Shaanxi Province of China (2022JM-023). We sincerely thank Prof. Xiao-Qiang Zhao for helpful discussions on mathematical modeling and the anonymous referees for many valuable suggestions. Li is in memory of his best friend, Wenjie, in the world.

References

COVID-19 Dashboard by the Center for Systems Science and Engineering (CSSE) at Johns Hopkins University (JHU), https://www.arcgis.com/apps/opsdashboard/index.html

Gatto M, Bertuzzo E, Mari L et al (2020) Spread and dynamics of the COVID-19 epidemic in Italy: effects of emergency containment measures. Proc Natl Acad Sci 117:10484–10491

Hu Z, Cui Q, Han J et al (2020) Evaluation and prediction of the COVID-19 variations at different input population and quarantine strategies, a case study in Guangdong province, China. Int J Infec Dis 95:231–240

Khan ZS, Bussel FV, Hussain F (2020) A predictive model for COVID-19 spread-with application to eight US states and how to end the pandemic. Epidemiol Infect 148:1–13

Kuniya T (2020) Prediction of the epidemic peak of coronavirus disease in Japan, 2020. J Chin Med 9:789

Lauer SA, Grantz KH, Bi Q et al (2020) The incubation period of coronavirus disease 2019 (COVID-19) from publicly reported confirmed cases: estimation and application. Ann Intern Med 172:577–582

Li Z, Zhang T, Gao J et al (2021) Preliminary prediction of the control reproduction number of COVID-19 in Shaanxi Province, China. Appl. Math J Chin Univ 36:287–303

Liu X, Huang J, Li C et al (2021) The role of seasonality in the spread of COVID-19 pandemic. Environ Res 195:110874

Liu Z, Magal P, Seydi O et al (2020) A COVID-19 epidemic model with latency period. Infect Dis Model 5:323–337

Munayco CV, Tariq A, Rothenberg R et al (2020) Early transmission dynamics of COVID-19 in a southern hemisphere setting: Lima-Peru: February 29th-March 30th. Infec Dis Model 5(2020):338–345

Musa SS, Wang X, Zhao S et al (2022) The heterogeneous severity of COVID-19 in African countries: a modeling approach. Bull Math Biol 84:1–16

Tang B, Bragazzi NL, Li Q et al (2020) An updated estimation of the risk of transmission of the novel coronavirus (2019-nCov). Infec Dis Model 5:248–255

Tang B, Wang X, Li Q et al (2020) Estimation of the transmission risk of the 2019-nCoV and its implication for public health interventions. J Chin Med 9:462

van den Driessche P, Watmough J (2002) Reproduction numbers and sub-threshold endemic equilibria for compartmental models of disease transmission. Math Biosci 180:29–48

World Health Organization, http://www.who.int/

Wang W, Zhao X-Q (2008) Threshold dynamics for compartmental epidemic models in periodic environments. J Dyn Differ Equ 20:699–717

Wang X, Wang H, Ramazi P et al (2022) From policy to prediction: forecasting COVID-19 dynamics under imperfect vaccination. Bull Math Biol 84:1–19

Wu J, Tang B, Bragazzi NL et al (2020) Quantifying the role of social distancing, personal protection and case detection in mitigating COVID-19 outbreak in Ontario. Can J Math Ind 10:15. https://doi.org/10.1186/s13362-020-00083-3

Xue L, Jing S, Miller JC et al (2020) A data-driven network model for the emerging COVID-19 epidemics in Wuhan, Toronto and Italy. Math Biosci 326:108391

Yan Q, Tang Y, Yan D et al (2020) Impact of media reports on the early spread of COVID-19 epidemic. J Theor Biol 502:110385

Yang Z, Zeng Z, Wang K et al (2020) Modified SEIR and AI prediction of the epidemics trend of COVID-19 in China under public health interventions. J Thorac Dis 12:165–174

Zhang F, Zhao X-Q (2007) A periodic epidemic model in a patchy environment. J Math Anal Appl 325:496–516

Zhang J, Litvinova M, Wang W et al (2020) Evolving epidemiology and transmission dynamics of coronavirus disease 2019 outside Hubei province, China: a descriptive and modelling study. Lancet Infect Dis 20:793–802

Zhang T, Li Z (2021) Analysis of COVID-19 epidemic transmission trend based on a time-delayed dynamic model. Commun Pur Appl Anal. https://doi.org/10.3934/cpaa.2021088
Zhao X-Q (2017) Dynamical systems in population biology, 2nd edn. Springer-Verlag, New York
Zhou L, Rong X, Fan M et al (2022) Modeling and evaluation of the joint prevention and control mechanism for curbing covid-19 in Wuhan. Bull Math Biol 84:1–26
Zou Y, Yang W, Lai J et al (2022) Vaccination and quarantine effect on COVID-19 transmission dynamics incorporating Chinese-spring-festival travel rush: modeling and simulations. Bull Math Biol 84:1–19